Automated Condition Monitoring for Helical Gears based on measuring Instantaneous Angular Speed with Magnetoresistive Sensors

Sebastian Pültz[1], Yannick Robin[1], Yanik Koch[2], David Quirnheim Pais[3], Lukas Rauber[3], Eckhard Kirchner[2], Andreas Schütze[1], Tizian Schneider[1]
1: Saarland University, Saarbrücken, Germany
2: Technische Universität Darmstadt, Germany
3: Sensitec GmbH, Wetzlar, Germany

Abstract

In this work, a novel approach is presented to extract physically motivated features for damage detection of gears in single-stage gearboxes by an automated order analysis of the instantaneous angular speed. This extraction method was applied to measurement data of various magnetoresistive sensors installed in a gearbox test bed and the obtained characteristics were examined in validation scenarios for their susceptibility to external disturbances. The classification results were compared to results obtained with an automatic Machine Learning (ML) method both on the data of the magnetoresistive sensors and an accelerometer. The new method has major advantages, especially with respect to transferability to other rotational speeds.

1 Introduction

In the context of Industry 4.0 and constantly increasing cost pressure, but also in the responsibility to use resources as efficiently as possible, predictive maintenance and full utilization of the service life of wear parts of complex modern machines are of major importance. Condition monitoring through data-based modelling is a central task here [1–3].

There are various possibilities to extract potentially relevant information from recorded sensor raw data. Typically, vibration sensors are used for condition monitoring [3]. However, many algorithms that analyse vibration data assume knowledge on the current rotational speed of the monitored component. In many applications this information can only be acquired by additional, e.g. magnetoresistive (MR) sensors. Therefore, it seems natural to use the MR sensor not only for speed measurement but also for the condition monitoring itself. This is possible by monitoring the effect of damages that cause fluctuations (in analogy to vibrations) in the instantaneous angular speed signal that can be derived from an MR angular decoder.

This will be demonstrated here using a helical gearbox in different damage states. It has been shown that the spectrum of the instantaneous angular speed (IAS) is superimposed by sidebands at the distance of the rotational frequencies of the connected shafts over the entire frequency range [4]. In the event of damage, these sidebands should increase in size [4]. However, the behaviour of a single sideband is often not very meaningful, so the overall behaviour of the sidebands should be investigated using statistical methods.

2 Dataset

The dataset consists of data recorded by five different sensors (see **Table 1**), including four different MR sensors concepts (Sensor A-D) and one accelerometer (Acc.) mounted in a single stage gearbox. The MR sensors measure the relative angle of the gear shaft with different measurement scales. The data of the MR sensors consist of two channels whose receivers are phase shifted by a quarter period. This results in a sine and cosine signal from which the current position, speed and direction of rotation can be determined. Further information about the employed sensors, data acquisition and preprocessing can be found in [5]. The signals from all MR sensors can be used to determine the IAS by first calculating the relative angle of the gear from the sine and cosine signals. Due to the knowledge of the sine and cosine values, the arctan2 function can be used to directly determine the current position of the shaft. This extends the tangent function, which is limited to the value range $]-\pi/2, \pi/2[$, to the interval $]-\pi, \pi]$ and thus enables a unequivocally statement about the position of the shaft. The derivation of this position signal then leads directly to the IAS signal [5].

Table 1 Overview of considered sensors [5]

Sensor	**Measuring scale**	Sampling rate
A	Straight toothed gear, $\boldsymbol{z3}$ = 51 teeth	100 kHz
B	Spur gear, $\boldsymbol{z2}$ = 95 teeth	40 kHz
C	Incremental pole ring, $\boldsymbol{z1}$ = 256 poles	40 kHz
D	Encoder magnet with north and south pole	40 kHz
Acc.		51.2 kHz

Two electric motors were connected to each side of the gearbox, one speed controlled, one torque controlled. For training data acquisition of the helical gear based on the IAS, four different parameters were varied during data acquisition (see **Table 2**). Primarily, artificial damage similar to pitting was introduced into a helical gear by milling and successively expanded. Furthermore, speed

ISBN 978-3-8007-5835-7

and load of the transmission were varied at six (speed) and seven (torque) levels using the connected electric motors. Finally, the load and direction of rotation were varied in negative and positive directions, resulting in four-quadrant operation [5].

Table 2 Parameters varied during data recording [5]

Parameter	Values	Interpretation
Damage	0	No Damage
	1	No Damage, removal and reinstallation
	2	Small pittings at one tooth flank
	3	Small pittings at three tooth flanks
	4	Bigger pittings at three tooth flanks
	5	Deeper pittings at three tooth flanks and over one entire flank
	6	Damage to three teeth over the entire flank
Speed	300, 700, 1000, 1300, 1600, 2000	min^{-1}
Torque	0, 20, 35, 55, 70, 85, 96	Nm
Quadrant	1	Motor 1 negative speed, Motor 2 positive torque
	2	Motor 1 negative speed, Motor 2 negative torque
	3	Motor 1 positive speed, Motor 2 negative torque
	4	Motor 1 positive speed, Electric Motor 2 positive torque

The data set consists of several measurements with different durations containing different combinations of the parameters described above. For data analysis one-second segments was extracted from each of these measurements resulting in a total of 923 segments. Segments with speed 1000 min^{-1} were not taken into account, firstly due to their low number and secondly because at this speed only damage class 0 is included in the data set.
For damage detection, the data set must be further reduced, since the damage was introduced into the flank on only one side of the teeth, and the damage is therefore only engaged in the correct combination of rotational direction and power flow direction. Therefore, only two quadrants can be considered: Quadrant 1 and Quadrant 4.

2.1 Evaluation Scenarios

Since one of the application goals is to keep the costs and thus the number of sensors used as low as possible, the sensors are evaluated individually to find the best suitable single sensor. Also, the evaluation scenarios were chosen to be as realistic as possible and to show robustness as well as statistical stability. Four different splits of the dataset were used for evaluation. For all evaluation scenarios, the goal was to distinguish between undamaged and damaged gears, so the segments were labelled according to damage class. Classes 0 and 1 were assigned the label OK, the remaining classes the label NOK. A second targeting vector, motivated later and included here only for completeness, further divides the NOK class into a more lightly damaged NOK 1 and a more heavily damaged NOK 2 class.
To minimize variance between test sets and thus avoid overfitting due to possible random unbalance of the test splits, a five-fold cross-validation (5-fold) was used.
Since all folds contain similar data in k-fold cross-validations, it is not possible to determine the influence of variable operating parameters like speed and torque on the classification result. In reality, these cross influences can cause domain shifts resulting in poorer model performance [6]. Therefore, two additional leave one group out cross validations were performed. First, the dataset was divided into folds based on speed to verify speed-independent detection of damages (Rpm). The second evaluation scenario is based on the classification according to the damage classes (Dam). Since the gears were removed each time in order to introduce further damage into the gear, the robustness of the model against a rebuild is also shown at the same time. Note, that this evaluation scenario results in highly unbalanced training and test data sets. Either the test fold consists only of OK data or it consists only of NOK data, which can easily lead to misinterpretation. To take this into account, a fourth evaluation scenario is introduced in which a hold-out evaluation generates a single train-test split in which the cycles of damage classes 0, 3 and 5 represent the test set and the segments from the remaining damage classes represent the train set (Hold-Out).

3 Methods

3.1 Automated ML-Toolbox

The raw data from the sensors and the IAS calculated from them were first analysed using an automated ML toolbox for condition monitoring [2,7]. This demonstrates the fully automated approach without explicit consideration of physical knowledge about the current rotational speed. The toolbox contains complementary approaches for dimensionality reduction in the form of feature extraction and feature selection as well as a classification via Mahalanobis distance following a projection by linear discriminant analysis (LDA). For this purpose, methods from the categories piecewise approximation, time domain transformations, frequency domain transformations, time-frequency domain transformations and statistical features are used for feature extraction. In addition to a simple Pearson correlation, feature selection is based either linearly separable (Recursive Feature Elimination Support Vector Machines, RFESVM [8]) or linearly non-separable (RELIEFF [9]) class divisions are used for selection. Pearson correlation between features and target vector is used for feature preselection to limit the number of features to 500 before applying RFESVM and RELIEFF. In the last step, an LDA is applied and the data is

ISBN 978-3-8007-5835-7

classified based on the Mahalanobis distance (see **Figure 1**[2].

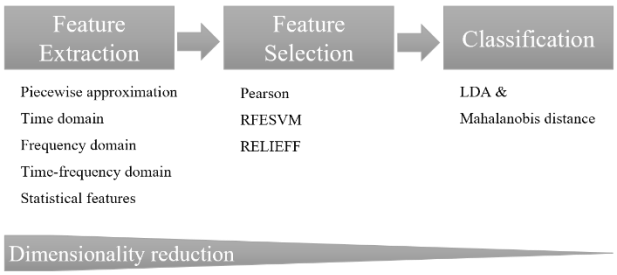

Figure 1 Schematic representation of the automated ML toolbox approach combining algorithms for feature extraction and feature selection for automated dimensionality reduction as well as classification

3.2 Feature Extraction from IAS Spectrum

To benchmark the explicit use of the additional speed information provided by MR sensors vs. the vibration sensor and the fully automated approach described above, a procedure was implemented that first automatically determined the rotational frequency and the tooth meshing frequency based on the MR sensors. Subsequently, the power spectral density was calculated, on the basis of which an automated order analysis was performed. Both the two raw signals and the IAS signal were included in the determination of the features.

The features that are now considered are calculated in a window around the MR sensors pole changing frequency for the sin and cos signals and for the IAS signal around the gear mesh frequency and their respective second to fifth harmonic. To statistically examine these windows, which extend ±10% of the determined frequency around the determined frequency, the statistical parameters root mean square (RMS), variance, kurtosis and skewness are determined, as well as the maximum value and the mean to max ratio. The second source of features is obtained from the absolute values of the sidebands at the distance of the rotational frequencies of the two shafts connected to the gearbox, around the pole changing frequency (sin, cos) and the gear meshing frequency (IAS) and their respective second to fifth harmonic, as well as the statistical moments of these values as described above.

Figure 2 shows, using sensor A as an example, which points and areas of the power spectral density are evaluated during feature extraction. The window in which the statistical moments are calculated is shown as well as the values of the sidebands. The sidebands in the IAS spectrum are much more recognizable than in the original sin or cos spectrum.

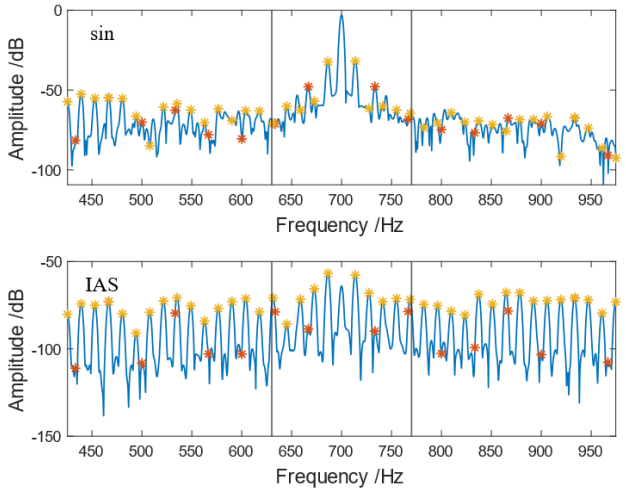

Figure 2 a) Sin Signal Spectrum of sensor A around pole changing frequency window from which the statistical moments were calculated (black lines), sidebands with distance of frequency of input gear (red), sidebands with distance of frequency of output gear (yellow); b) identical evaluation for the IAS spectrum of sensor A, both at 2000 min^{-1}, 0 Nm, Damage 0, Quadrant 1

It is therefore to be expected that the features obtained from the IAS spectrum contain more information than those from the spectra of the sensor raw data. It can also be clearly seen that the input shaft sidebands are barely visible, while those of the output shaft are clearly visible.

Principal Component Analysis was used to analyse the different influences of the experimental parameters on the features calculated as described above. To obtain clearer results, only the data of sensor A from the first quadrant are evaluated. The results are shown in **Figure 3**. Along the first principal component the rotational speed of the examined gear is evident in the physically plausible order. Even a larger separation of the 700 min^{-1} group compared to the other three groups is evident, indicating a nearly linear correlation between the first principle component and speed.

The second and third principal component represent the damage. Colouring the damage cases also shows clearly that the NOK data actually comprises two groups: the data of damage classes 2, 3 and 4 and those of classes 5 and 6 each form a cluster, while the third recognizable cluster contains the OK data. There seems to be significant difference between the calculated characteristics of the two NOK clusters, thus, the scenarios presented in chapter 2.1 are extended by running them once with the already known OK/NOK target and once with an extended target that divides the NOK group further into two separate classes. Based on the results of the principal component analysis, the NOK1 class contains the damage cases 2, 3 and 4 and the NOK2 class the damage cases 5 and 6.

ISBN 978-3-8007-5835-7

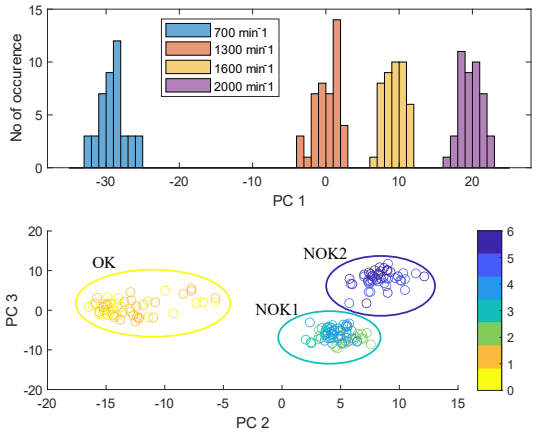

Figure 3 Variance of features for sensor A and quadrant 1 only: a) principal component 1 is strongly correlated with speed, b) principal components 2&3 (coloured in parameters from Table 2) indicate OK/NOK discrimination

4 Results

Initially, the evaluation scenarios described above were evaluated with data from quadrant 1 only, i.e., with the direction of rotation and power flow fixed. The transferability to the fourth quadrant will be checked separately at a later point of this chapter. In
Table 3 the performance of the ML toolbox for the individual evaluation scenarios and sensors is shown as benchmark. In all experiments, the scenarios were carried out with the two target labels, i.e. OK/NOK for the two class problem (2C) and OK/NOK1/NOK2 as extended three class problem (3C) also discriminating the damage severity. In general, the 2-class problem is much easier to detect than the 3-class problem extended by one damage level. Problems with transferability are particularly evident with the accelerometer when different velocities are involved (Rpm 2C and Rpm 3C).
Not surprisingly, classification with the MR sensor data shows major problems discriminating between the two NOK subclasses, when a variable parameter is not contained in the training data (Dam 3C, Rpm 3C). Thus, with the ML toolbox it is possible to detect if a gear is damaged, but the transferability is severely limited if the degree of damage is to be detected additionally.

Table 3 Evaluation results (Q1 only) with ML toolbox (accuracy in %)

	Acc.	A	B	C	D
5-fold 2C	100	100	100	100	100
5-fold 3C	97.7	87.5	89.8	97.2	80.1
Dam 2C	98.9	100	96.0	100	84.1
Dam 3C	92.6	69.9	71.0	88.6	56.8
Rpm 2C	79.0	100	96.6	100	97.7
Rpm 3C	69.3	83.5	77.8	68.8	75.6
Hold-Out 2C	100	100	100	100	100
Hold-Out 3C	93.4	75	80.3	86.8	68.4

Since it is assumed that the individual features obtained by the automated order analysis, especially the values of the sidebands, are highly correlated with each other, they are first preprocessed by standardization and principal component analysis. In order to be able to compare the classification results with the principal components obtained in this way with the ML toolbox, an internal 10-fold cross validation on the training data, performed iteratively with an increasing number of included principal components, is applied to determine how many principal components are required for ideal class separation. Note, that this internal CV does not affect the training-test splits applied in the respective evaluation scenarios.
For the 2-class problem (OK/NOK), similar accuracies to the ML toolbox are achieved, as indicated in **Table 4**. The main difference is obtained with the 3-class target OK/NOK1/NOK2 for sensor A. This sensor achieves similar results with nearly perfect accuracy across all experiments both for the 2-class and the 3-class problem. Reasons for this can be found in the significantly higher sampling rate of sensor A compared to the other sensors, but also its location, which is closest to the damage of all sensors.

Table 4 Evaluation scenario (Q1 only) results with IAS features (accuracy in %)

	A	B	C	D
5-fold 2C	99.4	97.7	100	97.2
5-fold 3C	99.4	79.6	76.1	79.0
Dam 2C	99.4	94.9	100	84.7
Dam 3C	99.4	53.4	79.6	59.7
Rpm 2C	99.4	94.3	100	97.7
Rpm 3C	99.4	72.7	84.7	76.7
Hold-Out 2C	96.8	100	100	99.0
Hold-Out 3C	98.7	73.7	76.3	67.1

Looking at the confusion matrix of the individual scenarios for the 3-class problem for the other sensors (e.g. sensor B, Dam scenario in **Figure 4**), it is clear that the low accuracy in these cases also results mainly from the failure to distinguish between the two damage subclasses, while the distinction between OK and NOK is still possible.
Finally, the transferability between quadrants 1 and 4 was checked. For this purpose, the evaluation scenarios already presented were combined with the data from Q1 and Q4. The classification results can be seen in **Table 5** for the ML toolbox and in **Table 6** for the IAS based feature extraction introduced in this work. For the automated order analysis, the data processing chain approach of principal component analysis, linear discriminant analysis and Mahalanobis distance as described above was chosen.

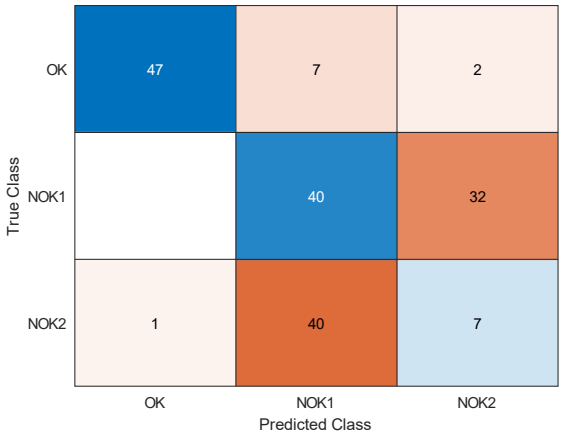

Figure 4 Confusion matrix for sensor B, scenario Dam 3C

As expected, the introduction of additional variability increases the complexity of the classification task. The significantly better results obtained for sensor A on the IAS signal again indicates that the rotation speed aware approach successfully reduces this complexity.

Table 5 Evaluation scenario (Q1 & Q4) results with ML toolbox (accuracy in %)

	Acc.	A	B	C	D
5-fold 2C	94.8	99.4	99.4	99.1	95.6
5-fold 3C	95.4	90.1	88.1	96.2	79.7
Dam 2C	86.3	96.5	94.2	87.5	91.3
Dam 3C	86.6	66.9	60.5	75.9	55.5
Rpm 2C	84	98.6	95.6	74.7	92.2
Rpm 3C	71.5	79.7	72.7	51.2	75.6
Hold-Out 2C	95.3	100	100	92.6	100
Hold-Out 3C	90.5	69.6	70.3	83.8	66.9

Table 6 Evaluation scenario (Q1 & Q4) results with IAS features (accuracy in %)

	A	B	C	D
5-fold 2C	98.0	98.8	89.0	93.6
5-fold 3C	99.4	78.2	86.9	77.0
Dam 2C	92.4	92.2	79.9	72.7
Dam 3C	90.4	46.8	76.2	50.9
Rpm 2C	95.6	81.7	82.3	91.0
Rpm 3C	93.9	73.3	80.8	71.8
Hold-Out 2C	97.8	99.5	88.1	97.8
Hold-Out 3C	99.3	64.9	81.1	67.6

5 Discussion and Conclusion

A significant advantage of MR sensors for condition monitoring of gears compared to accelerometers was shown, since they can explicitly take the rotational speed into account for damage detection without additional sensor.
The results suggest two assumptions on which parameters the quality of features obtained with automatic order analysis might depend. First, the classification results of sensor A suggest that its higher sampling rate provides an inherent advantage over the other MR sensors. Second, the results of sensors B-C suggest that sensors with a higher angular resolution of the sensor scale can also provide more information about the condition of the gear. It should be noted that sensor A was also placed closest to the damaged gear with its position on the counter-rotating gear. Further analysis and experiments are required to determine the importance of sampling rate, position and also noise level for the different sensors.
Similarly, a statistical estimate of the damage detection by the sidebands of the IAS spectrum seems possible. However, it should be further examined which of the characteristics described in chapter 3.2 actually have the greatest information content for the classification of the damage level.

6 Literature

[1] Schneider T, Helwig N, Schütze A. Industrial condition monitoring with smart sensors using automated feature extraction and selection. Meas Sci Technol 2018;29:094002. https://doi.org/10.1088/1361-6501/aad1d4.

[2] Schneider T, Helwig N, Schütze A. Automatic feature extraction and selection for condition monitoring and related datasets. 2018 IEEE International Instrumentation and Measurement Technology Conference (I2MTC), Houston, TX, USA: IEEE; 2018, p. 1–6. https://doi.org/10.1109/I2MTC.2018.8409763.

[3] Tiboni M, Remino C, Bussola R, Amici C. A Review on Vibration-Based Condition Monitoring of Rotating Machinery. Applied Sciences 2022;12:972. https://doi.org/10.3390/app12030972.

[4] Koch Y, Martin G, Kirchner E, Quirnheim Pais D, Slatter R. Feasibility study of measuring Instantaneous Angular Speed of Helical Gears with Magnetoresistive Sensors. International Conference on Gears (accepted), 2022.

[5] Koch Y, Georg M, Kirchner E, Qurinheim Pais D, Rauber L, Lenze T, Slatter R. Measurement of Instantaneous Angular Speed in a Helical Gear Box using Magnetoresistive Sensors, data set 2021. https://doi.org/10.48328/tudatalib-651.

[6] Goodarzi P, Schütze A, Schneider T. Comparison of different ML methods concerning prediction quality, domain adaptation and robustness. Tm - Technisches Messen 2022. https://doi.org/10.1515/teme-2021-0129.

[7] Dorst T, Robin Y, Schneider T, Schütze A. Automated ML Toolbox for Cyclic Sensor Data. Joint Virtual Workshop of ENBIS and MATHMET Mathematical and Statistical Methods for Metrology MSMM 2021, 2021.

[8] Guyon I, Elisseeff A. An Introduction to Variable and Feature Selection. Journal of Machine Learning Research 2003:1157–82.

[9] Kononenko I, Hong SJ. Attribute selection for modelling. Future Generation Computer Systems 1997;13:181–95. https://doi.org/10.1016/S0167-739X(97)81974-7.